ASTRONOMY & ASTROPHYSICS
SUPPLEMENT SERIES

Astron. Astrophys. Suppl. Ser. **144**, 181–186 (2000)

Application of the OS-EM method to the restoration of LBT images

M. Bertero[1] **and P. Boccacci**[2]

[1] INFM and DISI, Universitá di Genova, Via Dodecaneso 35, I-16146 Genova, Italy
[2] INFM and DIFI, Universitá di Genova, Via Dodecaneso 33, I-16146 Genova, Italy

Received October 13, 1999; accepted February 17, 2000

Abstract. The Large Binocular Telescope (LBT), which will be available in a few years from now, has been designed for high-resolution optical/infrared imaging through coherent cophasing of the two mirrors. The structure of the process of image formation in LBT is similar to that in Computed Tomography (CT) so that it is interesting to investigate the applicability to LBT of image restoration methods developed for CT. A powerful one is the so-called Expectation Maximization (EM), which is also known in the astronomical literature as Lucy-Richardson (LR) method. However slow convergence is a drawback of this method. In the case of CT an accelerated version, based on ordered subsets of projection data (OS-EM), has been proposed. In this paper we adapt OS-EM to the problem of restoring LBT images and we show that it provides an acceleration by a factor which is roughly equal to the number of independent interferometric images of the same object.

Key words: image processing, data analysis

1. Introduction

The Large Binocular Telescope (LBT) will consist of two 8.4 m mirrors on a common mount, with a 14.4 m centre-to-centre spacing. When the beams of the two mirrors are combined interferometrically the diffraction-limited resolution of this system in the direction of the baseline will be equivalent to that of a 22.8 m mirror. Moreover, thanks to the small distance between the mirrors, by taking images with different orientations of the baseline it is possible to have a coverage of the $u - v$ plane essentially equivalent to that of a 22.8 m mirror (Angel et al. 1998).

In order to exploit the imaging properties of LBT, the use of accurate image restoration methods will be required. This problem has been already considered by a few authors. For instance Hege et al. (1995) apply the iterative blind-deconvolution method developed by Jefferies & Christou (1993) to simulated LBT images of an extended object while Reinheimer et al. (1997) investigate the applicability to LBT of speckle masking and of the iterative building block method for the restoration of the object from its bispectrum (Hofmann & Weigelt 1993; Reinheimer et al. 1993).

More traditional restoration methods such as Tikhonov regularization, Conjugate Gradients (CG), projected Landweber method etc. (see, for instance, Bertero et al. 1995; Piana & Bertero 1996; Bertero & Boccacci 1998) have not yet been considered and we are preparing a paper on their extension to LBT images. However the extension of the Lucy-Richardson (LR) iterative method (Richardson 1972; Lucy 1974) has been used by Correia & Richichi 1999 for the restoration of simulated images and of LBT-like images taken at the TIRGO telescope. The results obtained by this method look good but the number of iterations required is exceedingly high.

The LR method is known as Expectation Maximization (EM) method (Shepp & Vardi 1982) in the literature on Computed Tomography (CT) where it is demonstrated that it provides reliable restorations both in PET and SPECT imaging. In the following we will use the denomination LR/EM for this method. Also in medical applications the number of iterations required for obtaining reliable restorations is too large. For this reason the acceleration of the method has been investigated by many authors. A very efficient technique, based on ordered subsets of projection data and called OS-EM method, has been proposed by Hudson & Larkin (1994). It provides the same accuracy as EM with a number of iterations which is smaller by a factor approximately equal to the number of subsets used by the algorithm, the computational cost of one iteration being essentially the same in EM and OS-EM.

It is interesting to point out that LBT imaging has a structure similar to that of CT imaging: a projection in CT provides information on the Fourier transform (FT)

Send offprint requests to: M. Bertero,
e-mail: bertero@disi.unige.it

of the object in the direction of the projection while an image of LBT provides information on the FT of the object mainly in the direction of the baseline. Therefore it looks quite natural to attempt the adaptation of OS-EM to LBT. This is the purpose of this paper. For simplicity we will restrict the analysis to the case of one image per orientation of the baseline and we will also assume that the number of orientations is small. Then it is quite natural to consider subsets consisting of just one image. The extension to the case of several frames per orientation angle or to the case of a continuously changing orientation is straightforward. In these cases one could also consider subsets consisting of more than one image and apply the strategies developed in the case of CT for the choice of the subsets (Hudson & Larkin 1994).

2. The LR/EM method for LBT imaging

We assume that p images of the same astronomical object, corresponding to p different orientations of the baseline, are available and that each image consists of $N \times N$ pixels, characterized by the indices m, n. We denote by $f(m,n)$ and $g_j(m,n)$ $(m,n = 0,1,...,N-1; j = 1,2,...,p)$ the values, at the pixel m,n, of the brightness distribution of the unknown object and of its j-th image, respectively. Moreover we denote by $\boldsymbol{f}$ and $\boldsymbol{g}_j$ the arrays formed by these values.

In the case of space-invariant PSF's the mathematical model of image formation is given by

$$g_j(m,n) = \sum_{m',n'=0}^{N-1} K_j(m-m', n-n') f(m',n') + w_j(m,n) \tag{1}$$

where $K_j(m,n)$ is the value, at the pixel m,n, of the PSF corresponding to the j-th orientation of the baseline and $w_j(m,n)$ is the value of the noise (Poisson noise, read-out noise etc.) corrupting the j-th image. We will write this equation in the following synthetic form

$$\boldsymbol{g}_j = \boldsymbol{A}_j \boldsymbol{f} + \boldsymbol{w}_j \tag{2}$$

$\boldsymbol{A}_j$ being, in general, a block-Toeplitz matrix which, as usual, can be approximated by a block-circulant matrix in order to easily compute matrix-vector products by means of FFT. This approximation is sufficiently good in many circumstances, and precisely when the size of the main lobe of the PSF is much smaller than the size of the image.

When the approximation of a periodic PSF is used, by computing the FFT of both sides of Eq. (2) we obtain the usual relationship

$$\hat{g}_j(m,n) = \hat{K}_j(m,n)\hat{f}(m,n) + \hat{w}_j(m,n). \tag{3}$$

The FFT of the PSF $K_j(m,n)$, i.e. $\hat{K}_j(m,n)$, is the *transfer function* of the system, corresponding to the j-th orientation of the baseline.

In order to formulate the LR/EM method for the restoration of LBT images in a compact form, let us define the product of two arrays $\boldsymbol{g}$ and $\boldsymbol{h}$, denoted by $\boldsymbol{gh}$, as the array which is obtained by multiplying each component of $\boldsymbol{g}$ by the corresponding component of $\boldsymbol{h}$, i.e. $(\boldsymbol{gh})(m,n) = g(m,n)h(m,n)$. Analogously the quotient $\boldsymbol{g}/\boldsymbol{h}$ is defined by $(\boldsymbol{g}/\boldsymbol{h})(m,n) = g(m,n)/h(m,n)$, provided that $h(m,n)$ is different from zero everywhere.

LR/EM is an iterative algorithm for approximating the solutions of the maximum likelihood problem in the case where images are corrupted by Poisson noise (Shepp & Vardi 1982). In such a case, if we assume that the images $\boldsymbol{g}_j$ are statistically independent and that their values at distinct pixels are also statistically independent Poisson processes, then the log-likelihood function is given by (except for a constant term depending on the images $\boldsymbol{g}_j$)

$$l(\boldsymbol{f}) = \sum_{j=1}^{p} \sum_{m,n=0}^{N-1} \{g_j(m,n) \ln[(\boldsymbol{A}_j\boldsymbol{f})(m,n)] - (\boldsymbol{A}_j\boldsymbol{f})(m,n)\}. \tag{4}$$

By means of the arguments developed by Shepp & Vardi (1982) it is easy to derive the LR/EM algorithm in the present case. The parameters related to the normalization of the columns of the imaging matrix, in the case of block-circulant matrices, are given by

$$\eta_j = \sum_{m,n=0}^{N-1} K_j(m,n) = \hat{K}_j(0,0). \tag{5}$$

so that, if we put

$$\eta = \sum_{j=1}^{p} \hat{K}_j(0,0), \tag{6}$$

the LR/EM algorithm is as follows

$$\eta \boldsymbol{f}^{(k+1)} = \boldsymbol{f}^{(k)} \sum_{j=1}^{p} \boldsymbol{A}_j^T \frac{\boldsymbol{g}_j}{\boldsymbol{A}_j \boldsymbol{f}^{(k)}}. \tag{7}$$

The iterations must be initialized with a positive image $\boldsymbol{f}^{(0)}$, the most simple choice being that of a uniform image.

It may be convenient to normalize the PSF's in such a way that $\hat{K}_j(0,0) = 1$. Then we get $\eta = p$. As follows from Eq. (3), this normalization implies that all quantities $\hat{g}_j(0,0)$ are equal, except for noise fluctuations, so that it can be consistently used if all images have essentially the same number of counts.

The usual properties of the EM algorithm can be easily extended to the present case: the result $\boldsymbol{f}^{(k)}$ of the $k-$th iteration is a non-negative estimate of the unknown object; in the case $\eta = p$ it satisfies the condition

$$\sum_{m,n=0}^{N-1} f^{(k)}(m,n) = \frac{1}{p} \sum_{j=1}^{p} \sum_{m,n=0}^{N-1} g_j(m,n), \tag{8}$$

i.e. the number of counts of the restored image is always equal to the arithmetic mean of the numbers of counts of

the images $\boldsymbol{g}_j$; $l(\boldsymbol{f}^{(k)})$ is an increasing function of k, so that, thanks to an argument due to Vardi et al. (1985), the iterates $\boldsymbol{f}^{(k)}$ converge to a maximum point of $l(\boldsymbol{f})$.

However it is important to remark that, as it is well-known, it is not convenient to push the algorithm to full convergence: too many iterations generate artifacts, mainly due to noise amplification, which reduce the quality of the restoration. In other words the maximum points of $l(\boldsymbol{f})$ do not provide sensible solutions. These can be obtained by a suitable stopping of the iterations since, as it may be shown by means numerical simulations, the number of iterations acts as a regularization parameter, in the sense that the method as a property which is often denoted as *semiconvergence*: the RMS error representing the discrepancy between $\boldsymbol{f}^{(k)}$ and $\boldsymbol{f}$ (the known object in the case of simulated images) first decreases for increasing k, remains approximately constant for a certain number of iterations and then grows again (Bertero & Boccacci 1998). An example of this behaviour will be given in Fig. 1.

This property implies that, for any given image, there exists an optimum number of iterations. In the case of real images it may be difficult to find this optimum number and this is the main shortcoming of the LR/EM method. This problem is even more important for the method we present in the next section because convergence (or semiconvergence) is faster. Indeed, in the case of LR/EM the minimum of the RMS error is, in general, rather flat and this property implies that, in the case of real images, one can stop the iterations when no significant modification is observed in the restoration. Another stopping rule may be provided by the so called *discrepancy principle*: the iterations are stopped when the RMS error representing the discrepancy between $\boldsymbol{A}_j\boldsymbol{f}^{(k)}$ and the observed image $\boldsymbol{g}_j$ becomes smaller than some estimated noise level.

3. The OS-EM method for LBT imaging

In the case of CT the modification of EM provided by OS-EM consists first in grouping the projections in ordered subsets and then in applying the standard EM algorithm to each subset, an iteration of OS-EM being a single pass through all the specified subsets. The application of OS-EM to LBT is obtained by replacing the projections with the images corresponding to different orientations of the baseline.

As we pointed out in the Introduction, we assume to have one image for each orientation angle and a small number of orientations. In such a case a quite natural choice is to take subsets consisting of one image, ordered, for instance, for increasing values of the parallactic angle corresponding to increasing values of the index j. Then the OS-EM method is as follows:

- initialize with $\boldsymbol{f}^{(0)}$ positive (for instance a uniform image);
- given $\boldsymbol{f}^{(k)}$ set $\boldsymbol{h}^{(0)} = \boldsymbol{f}^{(k)}$ and, for $j = 1, 2, ..., p$, compute

$$\eta_j \boldsymbol{h}^{(j)} = \boldsymbol{h}^{(j-1)} \boldsymbol{A}_j^T \frac{\boldsymbol{g}_j}{\boldsymbol{A}_j \boldsymbol{h}^{(j-1)}}; \tag{9}$$

- set $\boldsymbol{f}^{(k+1)} = \boldsymbol{h}^{(p)}$.

Again each iteration provides a nonnegative estimate of the unknown object, which, in the case of the normalizations $\hat{K}_j(0,0) = 1$ satisfies the condition

$$\sum_{m,n=0}^{N-1} f^{(k)}(m,n) = \sum_{m,n=0}^{N-1} g_p(m,n). \tag{10}$$

This condition does not coincide with but is essentially equivalent to condition 8 when the numbers of counts of the various images differ only by noise fluctuations. If large discrepancies are observed, it is possible to preprocess the various images in such a way that they have a number of counts coinciding with the arithmetic mean of Eq. (8). In this way it may be possible to avoid oscillations of the restored image inside one OS-EM iteration. Other methods for reducing these oscillations are proposed by Huang (1999).

As concerns the behaviour of the likelihood function $l(\boldsymbol{f}^{(k)})$, it has been observed by Hudson & Larkin (1994), in the case of numerical simulations, that it is in general an increasing function of k, so that also OS-EM should converge to a maximum point of $l(\boldsymbol{f})$, at least when the images are normalized in the way indicated above.

However the gain which can be obtained by means of OS-EM becomes evident only if one takes into account the semiconvergence property mentioned at the end of the previous section. Both EM and OS-EM have this property (as concerns OS-EM, see Hudson & Larkin 1994, where the RMS error is given as a function of the chi-square) but OS-EM reaches the best approximation of the unknown object after a number of iterations much smaller than that required by EM. As remarked by Hudson & Larkin (1994), in the case of nonoverlapping subsets the gain is by a factor of the order of the number of subsets. Therefore in our case the gain should be by a factor p, the number of images corresponding to different orientations of the baseline and this result is confirmed by the numerical simulations presented in the next section.

In order to appreciate the gain in computational time for the restoration of LBT images, it is important to remark that the computational cost of one LR/EM and one OS-EM iteration is approximately the same. As follows from Eq. (9), one OS-EM iteration consists of a cycle through all LBT images and therefore it requires the computation of the FFT's of the p arrays $\boldsymbol{h}^{(j)}$ in order to compute the denominators $\boldsymbol{A}_j\boldsymbol{h}^{(j-1)}$. On the other hand one LR/EM iteration requires the computation of the FFT of the array $\boldsymbol{f}^{(k)}$ for computing the denominators $\boldsymbol{A}_j\boldsymbol{f}^{(k)}$. It follows that one LR/EM iteration requires the computation of $3p + 1$ FFT's while one OS-EM iteration requires the computation of $4p$ FFT's. Therefore, if we assume

that the computation time is dominated by the number of FFT's, it follows that the time required by one OS-EM iteration is about 25% greater than the time required by one LR/EM iteration. For examples our IDL codes, running on a Pentium-200 MHz, requires 0.31 s per LR/EM iteration and 0.38 s per OS-EM iteration in the case of four 64×64 images.

4. Simulation study

We have tested the acceleration provided by OS-EM using some synthetic images generated by S. Correia and A. Richichi from Osservatorio Astrofisico di Arcetri. A complete description of these images is contained in Correia & Richichi (2000).

The first is a 128×128 image of the spiral galaxy NGC 1288. We have computed 4 sets of simulated observations, corresponding to $4, 6, 8$ and 10 equispaced values of the parallactic angle between 0° and 180° and to an integration time of 1000 s per parallactic angle. For these computations we have used ideal diffraction-limited PSF's, without taking into account the rotation of the baseline during the integration time nor the residual effect of the adaptive optics correction. The FWHM of these PSF's in the direction of the baseline was about 4 pixels. More realistic PSF models will be considered in future work. Finally each image has been corrupted by Poisson and read-out noise.

We have applied both LR/EM and OS-EM to each set of observations. The quality of the restoration provided by the k-th iteration has been measured by computing the relative RMS error defined as follows

$$\varrho^{(k)} = \frac{\|\boldsymbol{f}^{(k)} - \boldsymbol{f}\|}{\|\boldsymbol{f}\|} \tag{11}$$

where $\boldsymbol{f}$ is the original image of the galaxy and the norm is the Euclidean one.

In Fig. 1 we plot the behaviour of $\varrho^{(k)}$ as a function of k for the two methods (full line for LR/EM, dotted line for OS-EM) when $p = 8$. In both cases we find a minimum of the restoration error. The number of iterations corresponding to the minimum will be denoted by $k_{\rm opt}$. It is evident that $k_{\rm opt}$(OS-EM) is considerably smaller than $k_{\rm opt}$(LR/EM). The best restoration provided by OS-EM, which practically coincides with that provided by LR/EM, is shown in Fig. 2. All the results obtained in this example are summarized in Table 1 where $\varrho_{\rm min}$ denotes the minimum value of $\varrho^{(k)}$. Several interesting features of OS-EM result from this table.

First we observe that OS-EM provides the same restoration error as LR/EM. This restoration error is rather small, thanks to the high SNR assumed for the LBT images (the peak SNR is 80). As it must be, it decreases for increasing number of observations. Secondly the ratio between $k_{\rm opt}$(LR/EM) and $k_{\rm opt}$(OS-EM) is approximately p. As a result, while $k_{\rm opt}$(LR/EM) increases

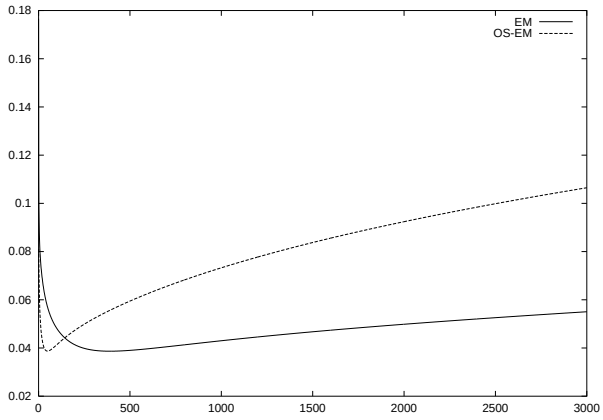

Fig. 1. Plot of the relative restoration error $\varrho^{(k)}$ as a function of the number of iteration k, both in the case of LR/EM (full-line) and in the case of OS-EM (dotted line). The case considered is that of 8 equispaced observations of the NGC 1288 galaxy

Table 1. Values of the minimum restoration error and of the corresponding number of iterations for various values of p both in the case of LR/EM and in the case of OS-EM. The example is the galaxy NGC 1288

p	$\varrho_{\rm min}$ (LR/EM)	$k_{\rm opt}$ (LR/EM)	$\varrho_{\rm min}$ (OS-EM)	$k_{\rm opt}$ (OS-EM)
4	4.4%	314	4.4%	79
6	4.0%	380	4.0%	64
8	3.9%	393	3.9%	50
10	3.5%	452	3.5%	46

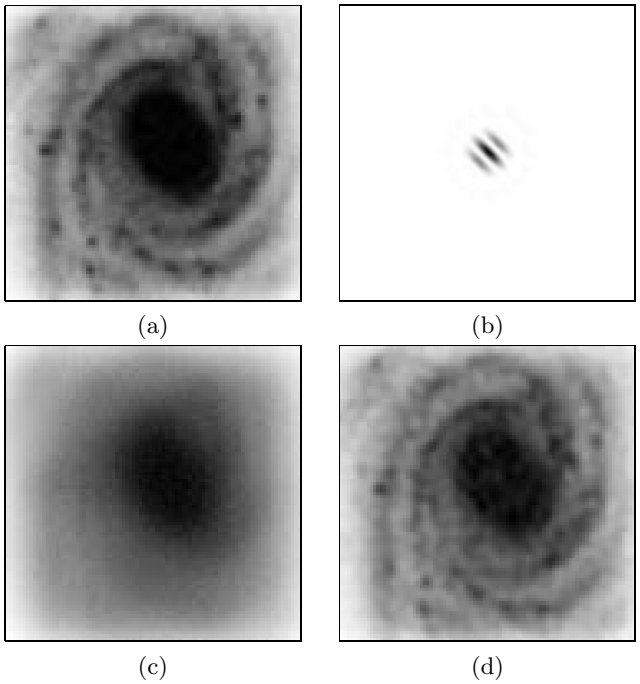

Fig. 2. a) Original image of the galaxy NGC 1288. **b)** One of the simulated LBT psf (parallactic angle = 67.5°). **c)** One of the simulated LBT images (parallactic angle = 0°). **d)** Restoration by means of 8 images, using the OS-EM method

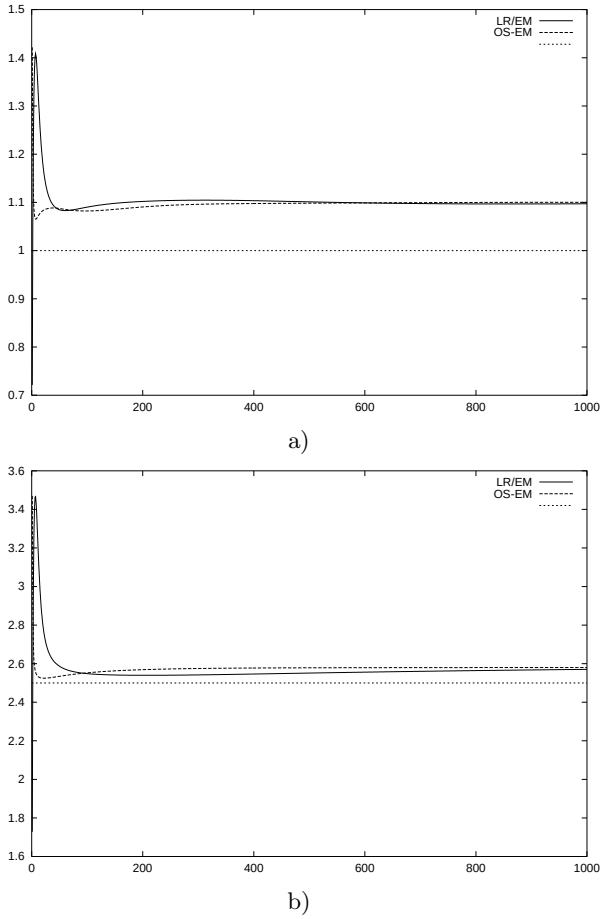

Fig. 3. Plot of the relative magnitude $\Delta m_{\rm r}$ as a function of the number of iterations both in the case of the LR/EM-method (full line) and in the case of the OS-EM method (dotted line). All the computations are performed using 8 different baselines. **a)** the case of binary stars with $\Delta m_{\rm r} = 2.5$. **b)** the case of binary stars with $\Delta m_{\rm r} = 1$

for increasing p, $k_{\rm opt}$(OS-EM) decreases. Since the computational cost of each iteration is roughly proportional to p, this result means that the computational cost of LR/EM rapidly increases for increasing p, while the cost of OS-EM increases very slowly.

The second example refers to binary stars of different relative magnitude. In the synthetic object each star is located in one pixel, with a separation between stars of about 14 pixels, which is about 3.5 times the *FWHM* of the *PSF's* in the direction of the baseline. Moreover two cases are considered: 1) the magnitudes of the two stars are 27.5 and 30 and the average peak SNR's in the image are 11.3 for the main star and 1.1 for the companion; 2) the magnitudes are 29 and 30 while the corresponding average peak SNR's are 5.5 and 2.2 respectively (Correia & Richichi 1999). Also for these examples we have computed sets consisting of $4, 6, 8$ and 10 equispaced observations.

These examples confirm that OS-EM provides an acceleration of LR/EM by a factor of p. However the convergence is much slower than in the example of the galaxy; a number of iterations of the order of thousand is required by LR/EM and, of course, a number of iterations of the order of hundreds by OS-EM. Our simulations confirm a well known feature of LR/EM: extended objects are recovered with a number of iterations smaller than that required for point-like objects.

As concerns the RMS restoration errors, they are higher than in the case of the galaxy, as a consequence of the smaller SNR: about 10% for example 1) and about $25 - 30\%$ for example 2). These RMS's are essentially unchanged if they are computed not on the complete image but on two square regions of 5×5 pixels centered on the positions of the two stars.

These simulations have also been used for comparing the astrometric and photometric performances of the two methods. Astrometric position is fully retrieved by both methods also in the case of the faint companion. Analogously both methods provide essentially the same photometric results. Indeed we performed aperture photometry on the restored images using 5×5 pixels regions centered on the brightest pixel of the reconstructed stars. In Fig. 3 we plot, as a function of the number of iterations, the relative magnitude for the restoration of the binary with $\Delta m_{\rm r} = 2.5$ (Fig. 3a) and of that with $\Delta m_{\rm r} = 1$ (Fig. 3b), both in the case of LR/EM (full-line) and in the case of OS-EM (dotted-line). The computations are performed using 8 images. The figures show that both methods provide essentially the same results after about 100 iterations. A more detailed discussion of photometry and of its dependence on the number of iterations and noise can be found in Correia & Richichi (1999).

5. Concluding remarks

In this paper we have extended the OS-EM method, which was introduced in computed tomography, to the restoration of LBT images. The method provides a considerable acceleration of the usual Lucy-Richardson method, denoted in this paper as LR/EM method. Indeed the computational cost of one iteration is approximately the same for the two methods but the number of iterations required by OS-EM is smaller than that required by LR/EM by a factor of the order of p, the number of LBT images corresponding to different orientations of the baseline. As a consequence, in the case of OS-EM the computation time for obtaining a reliable restoration is approximately independent of (or weakly dependent on) the number of LBT images. Moreover we have shown by means of numerical simulations that OS-EM and LR/EM provide in practice the same results as concerns the restoration errors and the evaluation of astrometric and photometric parameters.

Our IDL codes for the two methods are free and available on request to the authors.

Acknowledgements. This work was partially funded by CNAA (Consorzio Nazionale per l'Astronomia e l'Astrofisica) under the contract No. 16/97. We thanks Maurizio Busso, Mario Gai and Mario Lattanzi, from Osservatorio Astronomico di Torino, Serge Correia, Andrea Richichi and Piero Salinari, from Osservatorio Astrofisico di Arcetri, as well as Piero Calvini from Dipartimento di Fisica, Universita' di Genova, for several useful discussions and suggestions. We also thanks Serge Correia and Andrea Richichi for providing the images used in this paper to compare EM and OS-EM.

References

Angel J.R.P., Hill J.M., Strittmatter P.A., Salinari P., Weigelt G., 1998, in: Astronomical Interferometry, Reasenberg R.D. (ed.). Proc. SPIE 3352, 881

Bertero M., Boccacci P., 1998, Introduction to Inverse Problems in Imaging, Institute Of Physics, Bristol

Bertero M., Boccacci P., Maggio F., 1995, Int. J. Imag. Syst. Technol. 6, 376

Correia S., Richichi A., 2000, A&AS 141, 301

Hege E.K., Angel J.R.P., Cheselka M., Lloyd-Hart M., 1995, in: Advanced Imaging Technologies and Commercial Applications, Clark N., Gonglewski J.D. (eds.), Proc. SPIE 2566, p. 144

Hofmann K.-H., Weigelt G., 1993, A&A 278, 328

Huang S.-C., 1999, IEEE Trans. Nucl. Sci. 46, 603

Hudson H.M., Larkin R.S., 1994, IEEE Trans. Med. Im. 13, 601

Jefferies S.M., Christou J.C., 1993, ApJ 415, 862

Lucy L.B., 1974, AJ 79, 745

Piana M., Bertero M., 1996, J. Opt. Soc. Am. 13A, 1516

Reinheimer T., Hofmann K.-H., Weigelt G., 1993, A&A 279, 322

Reinheimer T., Hofmann K.-H., Scholler M., Weigelt G., 1997, A&AS 121, 191

Richardson W.H., 1972, J. Opt. Soc. Am. 62, 55

Shepp L.A., Vardi Y., 1982, IEEE Trans. Med. Imaging MI-1, 113

Vardi Y., Shepp L.A., Kaufman L., 1985, J. Amer. Statist. Soc. 80, 8